

A Statistic for identifying cosmic string wakes and other sheet-like structure

James Robinson and Andreas Albrecht

Blackett Laboratory, Imperial College
 Prince Consort Road, London SW7 2BZ U.K.

Abstract

We describe an implementation of the structure functions of Babul & Starkman [4], in order to quantify the “sheet-like” nature of a distribution of matter. We test this statistic on a toy model describing cosmic string wakes, and show that it does a better job than other statistics which have been proposed for distinguishing non-Gaussianity in the form of sheets. We conclude that the most favoured cosmic string model is unlikely to produce a significant increase in the sheet-like nature of the matter distribution beyond that which occurs in Gaussian models (with the same power spectrum) due to the formation of Zeldovich pancakes. Although the statistic was developed in the context of cosmic string wake formation, we expect it to be useful for comparing the observed galaxy distribution with a wide range of theoretical models with different power spectra.

Key words: cosmic strings – methods: statistical – dark matter – early universe – large scale structure of the universe.

1 Introduction

Advances in astronomy and theoretical physics are providing an increasingly detailed picture of the matter distribution in the universe, and of the predictions made by various theoretical models. Comparisons of theory with observations are made using statistics (such as the two-point correlation function) which might be able to identify significant differences or similarities among the models and data. Clearly, making the most of these comparisons involves identifying which are the most significant statistics to calculate.

Many models of primordial perturbations are “Gaussian”, and the density field at early times is completely characterized by the two-point correlation function (or power spectrum). However, on many scales we observe the matter distribution after the simple connections between the two point correlation function and other measurements have been destroyed by non-linear evolution.

The observed galaxy distribution exhibits many sheet-like features. So do essentially all of the theoretical models. Sheet-like behaviour is expected around scales where gravity is just going non-linear. A typical asymmetrical perturbation will collapse more quickly in one direction than the others, lending a sheet-like nature to the distribution of matter. In Gaussian models, the resulting sheet-like properties are a reflection of features of the initial power spectrum. It may well be that statistics sensitive to sheets are the best tool for exposing these features.

Wakes from cosmic strings can also produce sheet-like perturbations in the matter distribution. It is not yet clear whether in realistic cosmic string scenarios such wakes have a significant observational impact, or whether they are washed out by various competing factors. A statistic which is as sensitive as possible to sheet-like features will enhance our ability to address this question.

For this work, we constructed a toy model based on the cosmic string picture. We produced realizations of the matter distribution today based on a purely Gaussian set of primordial perturbations, and compared the results with the case where an individual cosmic string wake was added in “by hand”. By studying this toy model, we found an implementation of the structure functions of Babul & Starkman [4] which was better at identifying non-Gaussianity in the form of sheets than any other statistic we tried¹. We stress that although the cosmic string picture played a role in the development of this statistic, we expect its utility to extend beyond the cosmic string picture.

¹In an earlier version of this paper we found that a different measure of flatness was best at identifying wakes in our toy model. Since

The paper is organized as follows: The following section sketches our toy model and gives a qualitative discussion of the nature of the problem. Then Section 3 describes our implementation of the structure functions of Babul & Starkman, illustrates its application to the toy model, and compares it with other statistics. Section 4 gives our conclusions. Appendix A describes the toy model in detail. Appendix B describes a new “velocity coherence” criterion for the visibility of cosmic string wakes, and Appendix C describes how various two dimensional structures will show up in this statistic.

2 Qualitative look at our model and its output

2.1 The Toy Model

For the work described in this paper, we wanted a set of physically motivated models for the origin of large scale structure, which exhibit sheet-like properties in various degrees. Just such a set of models is described by Albrecht & Stebbins [2]. They consider density perturbations induced by three models of cosmic string (AT, I and X) in a background of HDM. To see how “wakey” the resulting perturbations are, they propose the following criterion: They ask whether the dominant contribution to the linear density contrast in a sphere of radius R centered on a wake comes from the wake (Δ_w) or from the Gaussian noise of other perturbations (characterized by an RMS value Δ_{rms}). The wake may be said to stand out if $\Delta_w \geq \Delta_{rms}$. In particular, they consider “maximal” wakes, which give the largest single contribution to linear density perturbations on a scale of 1Mpc. According to their criterion, maximal wakes in the X model stand out strongly, those in the I model are on the borderline, and those in the AT model do not stand out.

Our toy model works as follows: We consider the initial density perturbations induced in a box of side L to be made up of two components. Firstly, we take a realization of a Gaussian random field with a cosmic string power spectrum, as worked out by Albrecht & Stebbins [2]. Secondly, we add in the perturbation induced by a bit of string which enters the box when the coherence length of the string network is equal to the box size. Such a bit of string is approximately straight, and moves in an approximately straight line. We can therefore imagine it to seed a perturbation in a flat plane passing through the middle of the box. Having worked out the initial density field in our box, we evolve it to the present day using the adhesion approximation [13]. For consistency with the results presented for the three wakes models in [2], we use $h = 1.0$ throughout this paper. In Appendix A we describe our toy model in detail, and argue that it can give a fairly realistic picture of what wakes look like today.

2.2 Eyeball results

We have used our toy model to study maximal wakes (as discussed in the previous subsection) in the AT, I and X models. We chose to investigate these wakes as they also give the largest single contribution to the linear density contrast on a range of scales up to ~ 20 Mpc, and consequently have the best chance of being observed in the universe today. We note that the time these maximal wakes are laid down ($\eta = 6\eta_{eq}$) is independent of the network model we consider. Instead, it is a generic property of the HDM we are perturbing².

Results for boxes perturbed by wakes in each model are presented in a form suitable for examination by eye in Figure 1. Each picture shows a side view of all particles in the box, with the orientation chosen so that the plane which has been perturbed by the wake is seen end on, and occupies a vertical line through the middle of the picture. (These pictures were generated using 32^3 particles evolved on a 128^3 lattice). For comparison, we also show boxes evolved from the same Gaussian initial conditions, but where a wake has not been added. The boxes are 10Mpc, 20Mpc and 60Mpc respectively for the AT, I and X models³. The pictures for each model look similar because they are generated using the same random numbers. We see that only the X wake stands out clearly. In the I and the AT cases, there are new features in the boxes containing wakes. However, these features do not seem to be intrinsically different from the type of things which appear when the Gaussian alone undergoes collapse, and they certainly do not dominate the resulting density field.

There are two distinct reasons why X wakes stand out more than I and the AT wakes.

then we have developed a parallel version of our computer code, which has allowed us to scan a wider range of the parameter space available to the original statistic. Contrary to our original intuition, we have found that the wakes signal can be made even stronger by measuring the flatness of sections of the matter distribution which are several times smaller than the curvature scale of the wake. We find that these improvements have brought our statistic more in line with the use of the structure functions described by Babul & Starkman in [4].

²This fact has been employed in the past to use maximal wakes to model the entire impact of cosmic strings – see for instance Perivolaropoulos, Brandenberger & Stebbins [9]. However, this approach can only be valid if the maximal wakes stand out.

³Due to peculiarities in the “extreme” X model, the natural boxsize to choose is 60Mpc, approximately $\frac{2}{3}$ of the coherence scale.

Figure 1: AT, I and X boxes (top to bottom) with and without a wake (left to right).

1. *Properties of the initial density fields:* X wakes stand out more strongly in the initial density fields. According to the Albrecht and Stebbins wakiness criterion, both I and X wakes should stand out, but X wakes should stand out more. In Appendix B we propose a new visibility criterion for string wakes based on *velocity coherence* in initial density fields. Using this criterion, we demonstrate that there is not just a quantitative, but a *qualitative* difference between the manner in which X and I wakes stand out: X wakes dominate the bulk motions of matter, while I wakes do not. This prediction is borne out by an inspection of the pictures in this section.
2. *Effects of the non-linear evolution:* The degree of non-linear evolution in each box affects the visibility of the wakes. As we go from AT through I to X, we are looking at larger and larger boxes, because the coherence scale of the wakes at $\eta = 6\eta_{\text{eq}}$ is increasing. Consequently, we are looking at evolution which is less and less non-linear. Highly non-linear evolution will cause the wakes to break up into smaller objects, making them less continuous and harder to observe. Further, it produces other non-linear structures, such as Zeldovich pancakes, which provide competition against which the wakes may have difficulty standing out. So as we go from AT through I to X, the decrease in non-linearity of the evolution tends to increase the ease with which the wakes stand out.

The combination of these two effects allows the three cosmic string models to give an interesting range of cases to analyze. Since the I model is the best motivated by modern numerical simulations, the visual analysis suggests that individual string wakes will not play a dominant role in realistic string scenarios. We now turn to the problem of quantifying this issue.

3 Statistics

3.1 Counts in cells and the genus curve

The pictures in Figure 1 illustrate that maximal wakes laid down in the X model grow into significant structures today, and that those in the I and AT model have a small influence on matter distributions today. In this section we discuss how the resulting structures show up in *counts in cells* [10] and the *genus curve* [6], [7], both of which have been put forward as useful measures for identifying non-Gaussianity in the form of sheets [5]. In order to test these statistics, we compare their values for boxes evolved from the two types of initial conditions discussed earlier:

1. Realization of a strings power spectrum, plus a single string wake (as described in Appendix A).
2. Realization of a strings power spectrum on its own.

For the purposes of this paper, we only consider the idealized case where we have a well sampled map of the true density field. Issues concerning finite sampling effects and redshift-space distortion associated with real galaxy catalogues will be addressed in future work.

Results for the counts in cells statistic on our boxes for three different cell sizes are shown in Figures 2, 3 and 4. Here and throughout the paper, errorbars are shown at the 2σ level. A counts in cells analysis of the initial *linear* density contrast would yield plenty of information about the string wake, since an intrinsic effect of adding in the wake is to add a large Non-Gaussian component to the counts in cells distribution. However, as the field undergoes gravitational collapse, this information is lost, and the resulting probability distribution has the same form as we would expect for an evolved Gaussian field. We conclude that counts in cells is not a promising statistic with which to identify string wakes.

Discrete genus curves [5] for our boxes are shown in Figures 5, 6 and 7. None of the string models produce a strong signal in the curve. The point is made even more strongly in Figure 8, which shows genus curves for initial density fields generated by I and X string. Even for the initial density field, wakes only produce a tiny correction to the underlying Gaussian form of the genus curve. This suggests that the genus curve has little chance of picking out string wakes today.

Brandenberger et al. [5] argue on the basis of a different toy model that wakes produce a genus curve and a counts in cells distribution whose forms are qualitatively different from those which arise in other theories of structure formation. We feel that their wakes model tends to exaggerate the sheet-like features in the density field. On the other hand, our toy model might be underestimating the presence of sheets, at least in the X case (see Appendix A). In the end, a statistic will only be useful if it is effective in comparing observations and more realistic realizations of theoretical models. We expect that the enhanced sensitivity to wake-like features of the flatness statistic considered in the next subsection will make it a particularly useful tool.

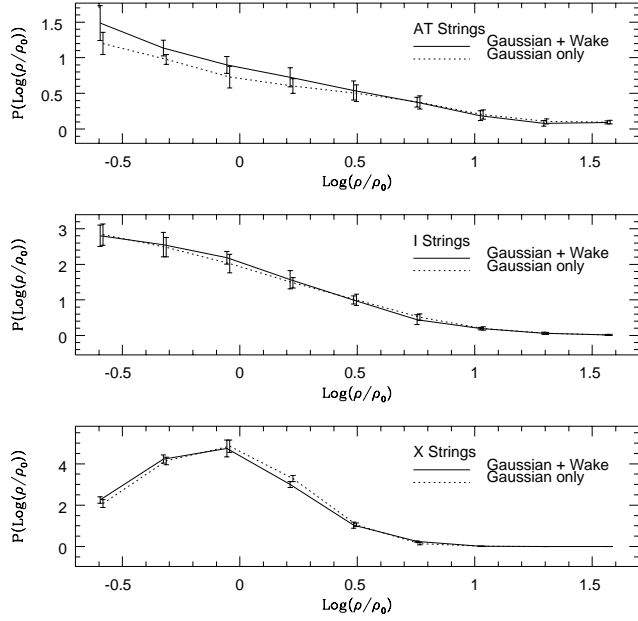


Figure 2: Counts in cells distributions for X, I and AT boxes with and without wakes. The boxes are 60Mpc, 20Mpc and 10Mpc respectively. In each case, the cell size is equal to the box size divided by 8.

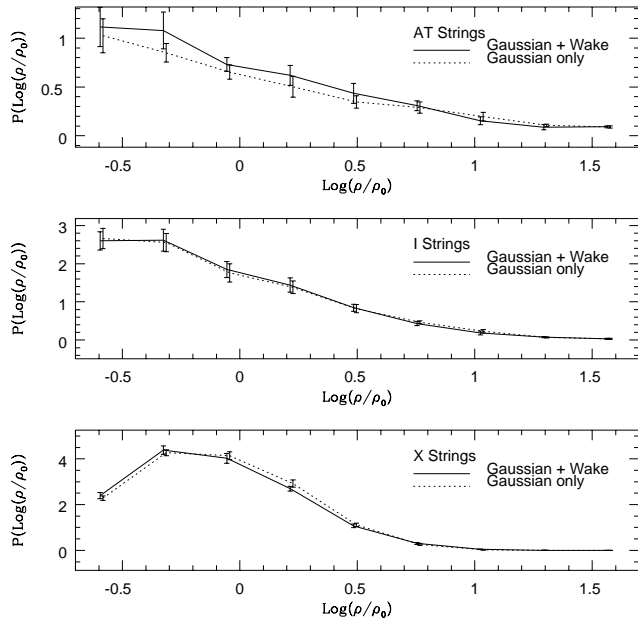


Figure 3: Counts in cells distributions for X, I and AT boxes with and without wakes. The boxes are 60Mpc, 20Mpc and 10Mpc respectively. In each case, the cell size is equal to the box size divided by 12.

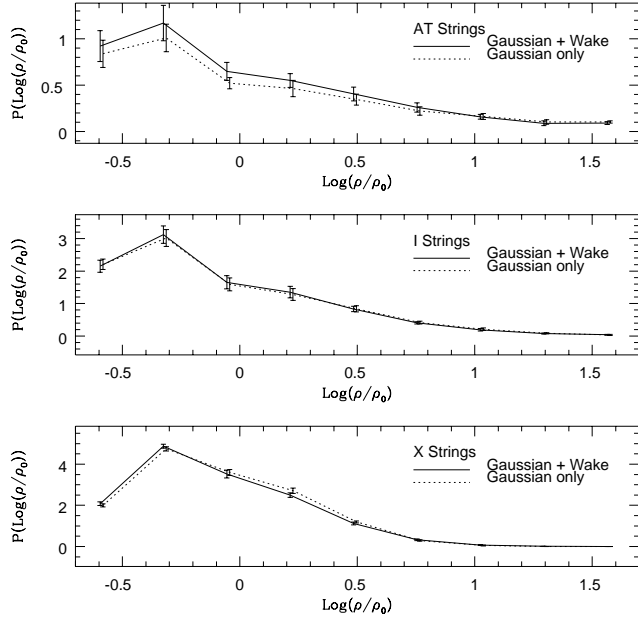


Figure 4: Counts in cells distributions for X, I and AT boxes with and without wakes. The boxes are 60Mpc, 20Mpc and 10Mpc respectively. In each case, the cell size is equal to the box size divided by 16.

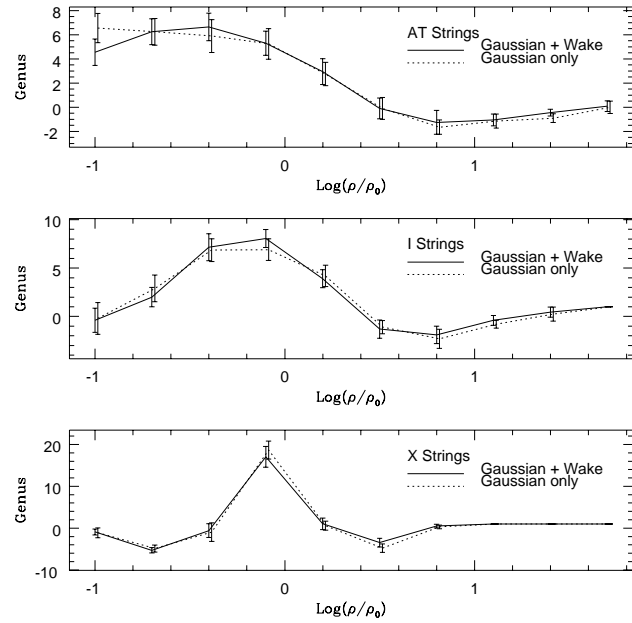


Figure 5: Discrete genus curves for X, I and AT boxes with and without wakes. The boxes are 60Mpc, 20Mpc and 10Mpc respectively. In each case, the cell size is equal to the box size divided by 8.

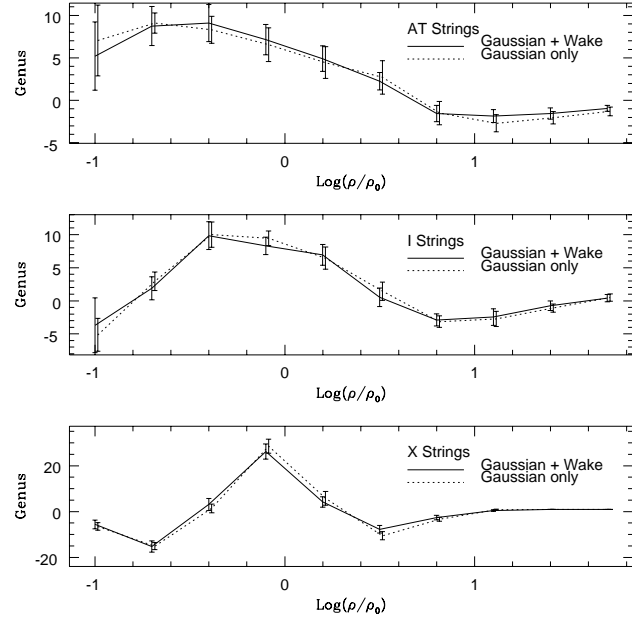


Figure 6: Discrete genus curves for X, I and AT boxes with and without wakes. The boxes are 60Mpc, 20Mpc and 10Mpc respectively. In each case, the cell size is equal to the box size divided by 12.

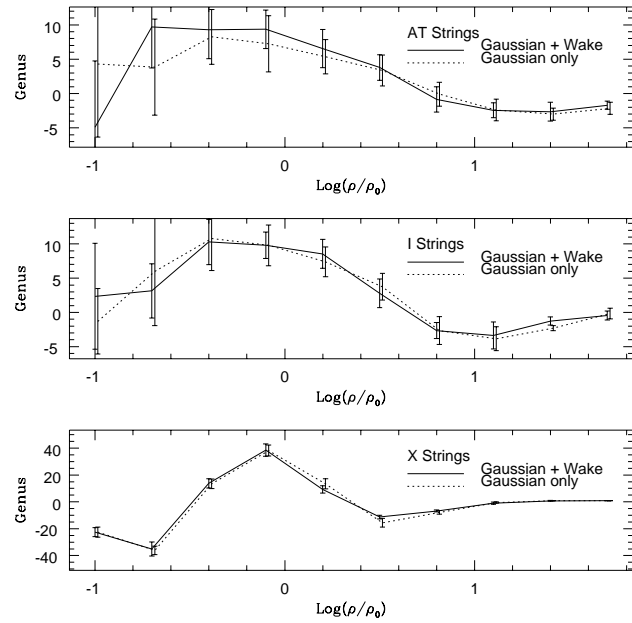


Figure 7: Discrete genus curves for X, I and AT boxes with and without wakes. The boxes are 60Mpc, 20Mpc and 10Mpc respectively. In each case, the cell size is equal to the box size divided by 16.

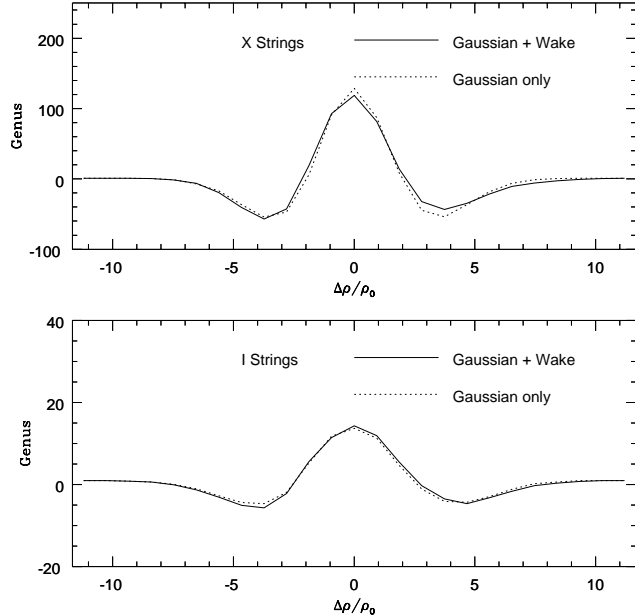


Figure 8: Discrete genus curves for initial X and I boxes with and without wakes. The boxes are 60Mpc and 20Mpc respectively. In each case, the cell size is equal to the box size divided by 16. Isosurface cutoffs are normalized to the present day using linear gravity.

3.2 Looking for wakes via flatness

In this subsection, we discuss statistics which might identify wakes via their morphology. First, we consider an implementation of the structure functions of Babul & Starkman [4]. The structure functions S_1 , S_2 & S_3 are a set of measures quantifying the shape of an object. They take the value 1.0 for a perfect filament, plane or sphere respectively, and they fall off rapidly to 0.0 as the object deviates from each of these forms.

The starting point for these measures is the inertia tensor. For an object consisting of a collection of point masses this is defined as

$$I_{ij} = M_{ij} - M_i M_j \quad (1)$$

where

$$M_i = \frac{1}{M} \sum_k m^{(k)} r_i^{(k)} \quad (2)$$

$$M_{ij} = \frac{1}{M} \sum_k m^{(k)} r_i^{(k)} r_j^{(k)} \quad (3)$$

$$M = \sum_k m^{(k)} \quad (4)$$

and $m^{(k)}$ is the weight of the k^{th} point. Taking I_1 , I_2 , I_3 to be the eigenvalues of I_{ij} in decreasing order of magnitude, S_1 , S_2 & S_3 are defined as follows:

$$S_1 = \sin \left[\frac{\pi}{2} (1 - \nu)^p \right] \quad (5)$$

$$S_2 = \sin \left[\frac{\pi}{2} a(\mu, \nu) \right] \quad (6)$$

$$S_3 = \sin \left(\frac{\pi \mu}{2} \right) \quad (7)$$

where

$$\nu = \left(\frac{I_2}{I_1} \right)^{1/2} \quad (8)$$

$$\mu = \left(\frac{I_3}{I_1} \right)^{1/2} \quad (9)$$

$$p = \frac{\log 3}{\log 1.5} \quad (10)$$

and $a(\mu, \nu)$ is defined implicitly by

$$\frac{\nu^2}{a^2} - \frac{\mu^2}{a^2(1 - \alpha a^{1/3} + \beta a^{2/3})} = 1 \quad (11)$$

with

$$\alpha = 1.9 \quad (12)$$

$$\beta = -\frac{7}{8}9^{1/3} + \alpha 3^{1/3} \quad (13)$$

In addition, we consider a new flatness measure F , defined as

$$F = \frac{\sqrt{3}(I_2 - I_1)(I_1^2 + I_2^2 + I_3^2)^{1/2}}{(I_1 I_1 + I_1 I_2 + I_1 I_3 + I_2 I_2 + I_2 I_3 + I_3 I_3)} \quad (14)$$

This measure is chosen to take the value 1.0 for a perfect plane, but to fall away less rapidly to 0.0 than S_2 as the object deviates from planarity. In Appendix C we compare the values of F and S_2 for sections of a spherical shell, which may model realistic wakes better than a perfect plane.

In order to apply these statistics to a density field, we first need to first identify objects in that field to measure the shapes of, and then to employ some method of averaging over the quantities obtained for these objects. Babul & Starkman [4] illustrate two important criteria for the identification of objects.

- *Scale*: Firstly, they illustrate the strong dependence of S_1 , S_2 and S_3 on the length scale on which objects are picked out of the distribution.
- *Thresholding*: Secondly, they show that the quantitative signal of an object can be made stronger by “thresholding”, that is, by throwing away those parts of the matter distribution where the local density is below some cutoff value⁴.

We adopt the following scheme for identifying objects in our matter fields, which incorporates both of these criteria.

We divide our distribution into $i = 1 \dots N$ cubes, C_i , of side R_{smooth} . We introduce thresholding by associating a mass m_i with the centre of each cube, which is a function of the density inside that cube ρ_i , and some cutoff density ρ , as follows.

$$m_i = \rho \theta(\rho_i - \rho) \quad (15)$$

where

$$\theta(x) = \begin{cases} 0 & \dots x < 0 \\ 1 & \dots x \geq 0 \end{cases} \quad (16)$$

For each of the M cubes C_i for which the density ρ_i is above the threshold, we construct an object O_i which is the set of all cubes C_j contained within a cube of side R centered on C_i . (In order that we always deal with whole cubes, R will be some integer multiple of R_{smooth}). For each object O_i we work out the structure functions and the flatness statistic S_1^i , S_2^i , S_3^i and F^i . We then compute the average values $S_1 = \frac{1}{M} \sum_i S_1^i$ etc, providing a set of four numbers S_1 , S_2 , S_3 and F which quantify the morphology of the density field, as a function of the three parameters ρ , R and R_{smooth} .

In order to consider a wide range of parameter space, we have developed a parallel computer code, and we present our results as “shapes curves”, showing the variation of S_1 , S_2 , S_3 and F with ρ , for given values of R . In Figures 9,10 and 11 we present a selection of results for the X and I string models, with various choices for the parameters. All errorbars are shown at the 2σ level. In order to present our results in a manner which is independent of the degree of non-linear evolution in each of the models, for each cutoff ρ we plot the volume fraction V of cubes C_i in the distribution for which $\rho_i > \rho$. We see that for a suitable choice of parameters ($V \sim 0.05$, $R \sim 11\text{Mpc}$) we can distinguish boxes with and without X string wakes at the 2σ level. However, none of the measures can distinguish boxes with and without wakes in the I and AT models. We note that both S_2 and F are capable of picking out

⁴An alternative method for amplifying the signal of an object is the minimal spanning tree. This technique has been investigated by Pearson and Coles[8]. It would be interesting to apply this technique to the density fields considered in this paper.

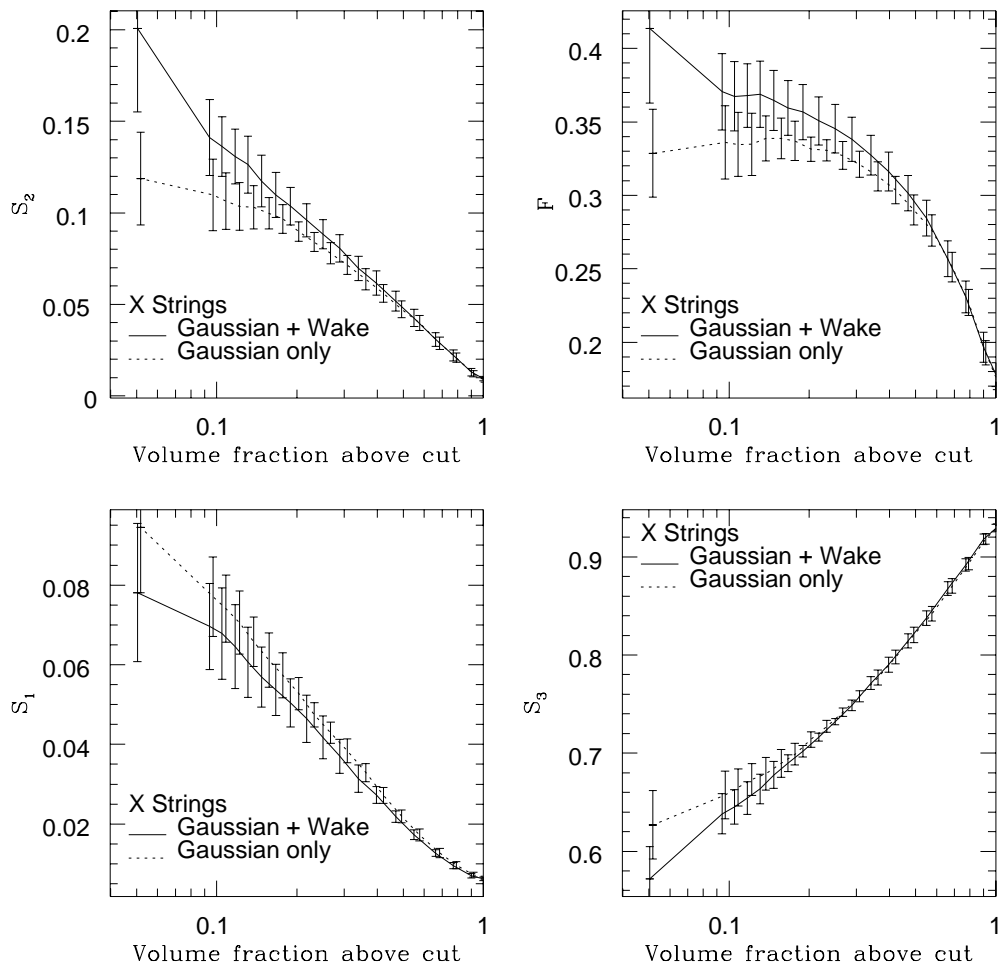


Figure 9: Shapes curves for 60Mpc boxes in the X string model. R is $\frac{3}{16}$ of the boxsize, and R_{smooth} is $\frac{1}{16}$ of the boxsize.

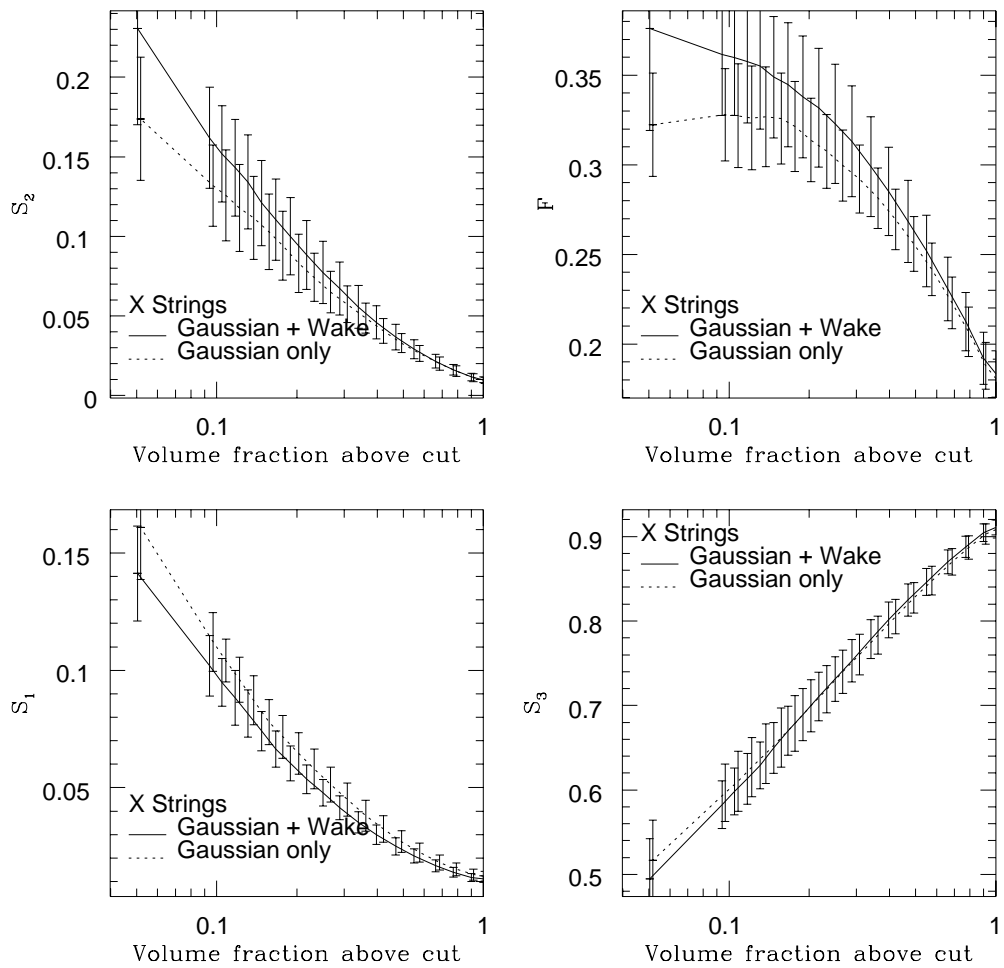


Figure 10: Shapes curves for 60Mpc boxes in the X string model. R is $\frac{7}{16}$ of the boxsize, and R_{smooth} is $\frac{1}{16}$ of the boxsize.

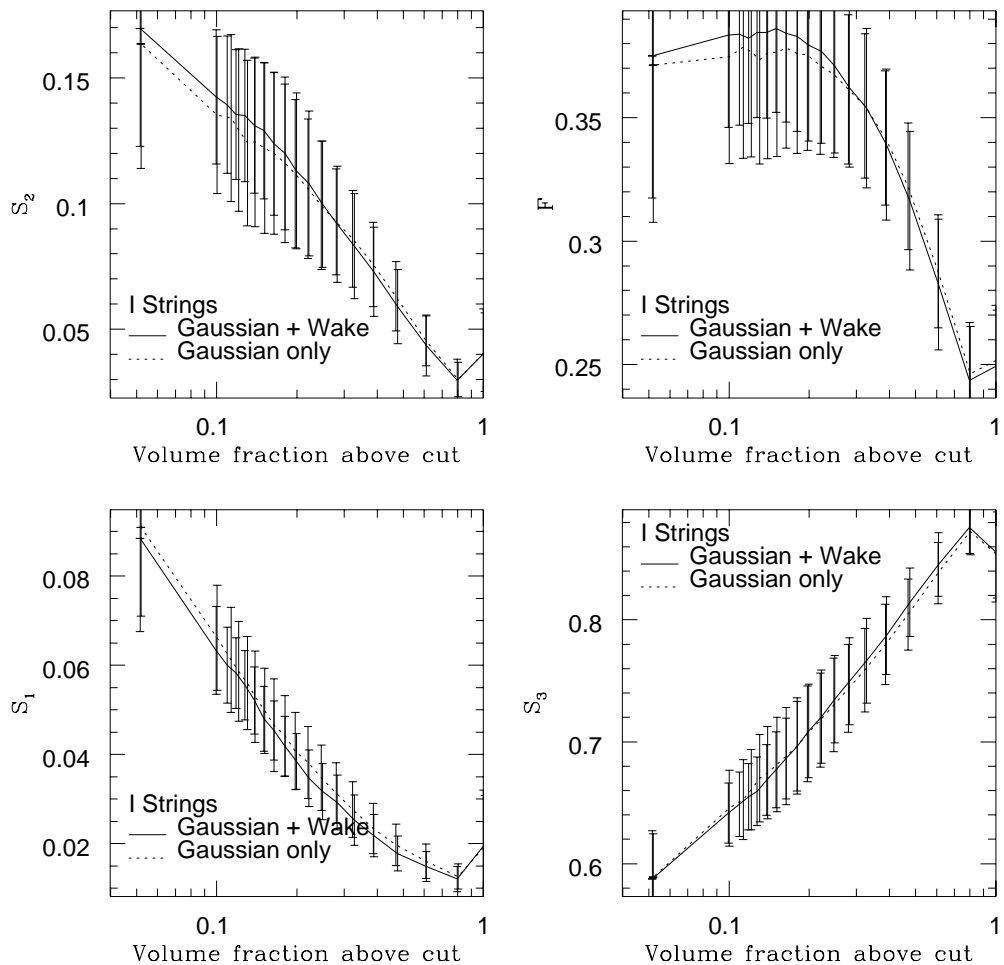


Figure 11: Shapes curves for 20Mpc boxes in the I string model. R is $\frac{3}{16}$ of the boxsize, and R_{smooth} is $\frac{1}{16}$ of the boxsize.

idealized flat X wakes at the 2σ level, with S_2 performing slightly better. However, we anticipate that the quantity F may perform better than S_2 when picking out features which are not exactly flat (See Appendix C). As expected, the measures S_1 and S_3 which quantify filamentarity and sphericity respectively are not useful for distinguishing wakes.

We stress that the model we have used to generate density fields is only a *toy* model. We do not know whether string wakes will stand out more or less than this in realistic models. If they stand out a little bit more, then the statistic may be a useful tool for identifying them. If they stand out less, then any statistic will have difficulty in distinguishing them from the collapsed remnants of a Gaussian distribution. In general, it seems that wakes which only just show up in initial density fields (in particular, those that stand out on the linear gravity criterion but fail to stand out on the velocity coherence criterion – see Appendix B) tend to disappear under non-linear gravitational evolution. This observation may well be of importance when assessing the wakiness of realistic models.

Although we have tested the flatness statistic on a toy model for cosmic string wakes, we also expect it to be useful for distinguishing models with different Gaussian initial conditions. As a density field undergoes gravitational collapse, it becomes harder to retrieve information about the linear initial conditions which have given rise to that collapse. This point is easily visualized in the adhesion approximation, where degrees of freedom present in the initial positions and velocities of particles are lost as the particles stick together. For a whole range of initial conditions, the first objects formed by gravitational collapse are Zeldovich pancakes. It is possible that the hard-to-retrieve information about linear initial conditions is best encoded by these pancakes. The problems involved in identifying and quantifying these pancakes are similar to those involved in identifying X string wakes: From the discussion in the previous subsection, we expect that a flatness curve based on objects contained by isosurfaces will provide a good way of identifying these features.

4 Discussion and Conclusions

We have tried out various measures of the sheetiness of a distribution of matter, using a toy model of cosmic string wakes in HDM. In the most realistic version of our toy model (with an “I” string network) we find that it is not possible to pick out single wakes. However, our toy model is rather simplistic and it will be interesting to see the extent to which improved models of the string network might give a different result. If anything, our model makes the wakes unrealistically flat, and our expectation is that a more realistic model will make the wakes less noticeable.

We have shown that wakes which fail to satisfy our velocity coherence criterion (see Appendix B) at the linear stage tend to stand out less as a field undergoes non-linear gravitational evolution. We believe that this observation will help simplify assessing the wakiness of more realistic string models.

We have also investigated an extreme (“X” string) model, where the wakes *do* stand out strongly today. We have demonstrated that a good choice of statistic is required to find the wakes, even in this case. Counts in cells, the discrete genus curve, and some flatness statistics, do not pick out the wakes well. However, we have found that the “flatness curve”, based on the structure function S_2 of Babul & Starkman, produces a strong wakes signal. The adhesion approximation we use for gravity is known to exaggerate the extent to which the Zeldovich pancakes are sheet-like. Thus our work might underestimate the differences between these pancakes and wakes.

We have shown that the flatness curve is a good statistic for identifying X wakes (see Section 3.2), and expect that it will also be useful for identifying other types of sheet-like structure. We note that some properties of any initial density field (including Gaussian fields) may be best encoded in the “pancakey” nature of the evolved distribution. Hence, the flatness curve could well be a useful tool for discriminating between many types of theories for the origin of large scale structure.

5 Acknowledgements

We would like to thank Pedro Ferreira and Julian Borrill for helpful discussions. We are also grateful for the use of the AP1000 at the IC-Fujitsu Parallel Computing Research Centre.

References

- [1] Albrecht A., Stebbins A., 1992a, Phys. Rev. Lett., 68, 2121
- [2] Albrecht A., Stebbins A., 1992b, Phys. Rev. Lett., 69, 2615
- [3] Albrecht A., Turok N., 1989, Phys. Rev. D, 40, 973

- [4] Babul A. Starkman G.D., 1992, ApJ, 401, 28
- [5] Brandenberger R.H., Kaplan D.M., Ramsey S.A., 1993, astro-ph/9310004
- [6] Gott J., Melott A., Dickinson M., 1986, ApJ, 306, 341
- [7] Gott J., Weinberg D., Melott A., 1987, ApJ, 319, 1
- [8] Pearson R.C., Coles P., 1995, MNRAS, 272, 231
- [9] Perivolaropoulos L., Brandenberger R.H., Stebbins A., 1990, Phys. Rev. D, 41, 1764
- [10] Salsaw W., 1989, ApJ, 341, 588
- [11] Stebbins A., 1990, in Gibbons G., Hawking S., Vachaspati T., eds, The Formation and Evolution of Cosmic Strings, Cambridge University Press, Cambridge, p. 503
- [12] Vishniac E., 1986, in Kolb E.W., Turner M.S., Lindley D., Olive K., Seckel D., eds, Inner Space Outer Space. University of Chicago Press, p. 190
- [13] Weinberg D.H., Gunn J.E., 1990, MNRAS, 247, 260

A The Model

Our picture of how cosmic string wakes are laid down can be visualized in terms of the *one scale* model of string network evolution [3]⁵. In the one scale model, the statistics of the evolving network are specified by one comoving scale ξ , a monotonically increasing function of conformal time η , which characterizes the mean inter-string separation, mean string curvature, and the mean step size of the string walks. Suppose we lay down comoving boxes of side L at random in the universe and want to work out how the string network perturbs the matter in these boxes between its formation at time η_i , and the present day η_0 . If we define η_L to be the time at which $\xi(\eta_L) = L$, then we can separate the perturbation history of the boxes into three epochs:

1. $\eta_i < \eta < \eta_L$. In this epoch, the string network describes random walks with step size less than the box size. We approximate the resulting perturbation as a Gaussian random field, whose power spectrum may be worked out using the method of Albrecht & Stebbins [1]. (For the purposes of our toy model we have considered perturbations in the HDM background described by Albrecht & Stebbins [2], with $h = 1.0$, $\sigma_8 = 1.0$ and no bias). Since we are only interested in perturbations seeded before time η_L , we truncate the integration at $\eta = \eta_L$. So

$$P(k) = 16 \pi^2 \frac{(1 + z_{\text{eq}})^2}{(1 + z_m)^2} \mu^2 \int_{\eta_i}^{\eta_L} |T(k, \eta)|^2 F(k, \eta) d\eta \quad (17)$$

Here, z_m is the redshift at some time in the matter era to which we can evolve the perturbations using linear gravity.

Clearly, as the time approaches η_L , the perturbations produced in this epoch become more and more sheet-like on the scale of the box. The question of whether approximating all these perturbations as Gaussian random noise is realistic can be assessed by seeing how much the single wake we add stands out. For AT and I strings, the wake stands out very little, so the approximation is good. For the X model, the wake stands out strongly, so the approximation may be unreasonable.

2. $\eta_L < \eta < \eta_L + \Delta\eta$. Here ξ is of order L , so strings in the boxes look roughly straight and move in roughly straight lines. Consequently, wakes laid down in any of the boxes look roughly planar. The length of time $\Delta\eta$ required to generate a box sized portion of one of these wakes is given by $\Delta\eta = L/v_b$, where v_b is the macroscopic bulk velocity of a section of string in the network. Now, we can also estimate the *total* area of string wakes generated in this time per unit volume of universe. At any time, the length of string per unit volume of universe is equal to ξ^{-2} . So in a time interval $d\eta$ the area of wake traced out per unit volume is

⁵ Inadequacies in the one scale model have been exposed by high resolution numerical simulations and a recently developed three scale model attempts to address some of these inadequacies. It would be interesting to investigate how deviations from the one scale picture could change our conclusions, but we expect the corrections to be small.

$v_b \xi^{-2} d\eta$. Consequently, the total wake area traced out per unit volume between times η_L and $\eta_L + \Delta\eta$ is given by

$$a_2 = v_b \int_{\eta_L}^{\eta_L + \Delta\eta} \frac{d\eta}{\xi^2} \quad (18)$$

Consider the X string model, where $\xi(\eta) = \eta$. Then

$$a_2 = v_b \left(\frac{1}{\eta_L} - \frac{1}{\eta_L + \Delta\eta} \right) = \frac{v_b}{L(v_b + 1)} \quad (19)$$

Every time a box hits a wake, the area of wake per unit volume contained in the box is of order $L^2/L^3 = L^{-1}$. Let the fraction of boxes hitting wakes laid down in this epoch be p_2 . Then equating string area per unit volume over an ensemble of boxes we have

$$\frac{p_2}{L} = \frac{v_b}{L(v_b + 1)} \quad (20)$$

Hence we can work out

$$p_2 = \frac{v_b}{1 + v_b} \quad (21)$$

(The results for I and AT models will be similar). Then the perturbations in this epoch are well approximated as follows

- (a) A fraction p_2 of the boxes are perturbed by a single string, which by an appropriate choice of axes we may take to have moved in a straight line through the middle. To work out the density perturbation we simply calculate $\theta_+(k, \eta)$ for a straight string moving in a straight line through the middle of the box, and substitute into equation (2) of [1]. We use $v_b = 0.3$ for the AT and X models, and $v_b = 0.15$ for the I model. The difference reflects the enhanced small scale structure in the I model.
- (b) A fraction $1 - p_2$ of the boxes do not undergo any perturbations in this epoch.

3. $\eta_L + \Delta\eta < \eta < \eta_0$. The area of wakes per unit volume generated in this epoch is given by

$$a_3 = v_b \int_{\eta_L + \Delta\eta}^{\eta_0} \frac{d\eta}{\xi^2} \quad (22)$$

which for $\eta_0 \gg \eta_L$ in the X model works out to

$$a_3 = \frac{v_b^2}{L(v_b + 1)} \quad (23)$$

ξ is now greater than L , so wakes laid down in any of the boxes look very planar. Hence, the area of wake per unit volume in any box which hits a wake is approximately L^{-1} . Let the fraction of boxes hitting wakes laid down in this epoch be p_3 . Doing the same calculation as in the last epoch, we see that $p_3 = \frac{v_b^2}{(v_b + 1)}$, which is always less than 0.5, and may be as low as .019 if $v_b = 0.15$. So the majority of boxes, a fraction $1 - p_3$, undergo no perturbations in this epoch. We will consider only these boxes. (Again, results will be similar for the AT and I models).

This picture provides a simple way of working out what the wakes laid down at time η_L will look like today: Provided η_L lies in the regime where linear gravity is a good approximation, we can choose some later time η_M in the matter dominated era of the universe, at which linear gravity is still a good approximation. We can work out perturbations induced during Epoch 1 at time η_M by computing a realization of the power spectrum in Equation (17). We can work out perturbations induced during Epoch 2 using Equation (2) of [1]. Up to time η_M gravity is still linear so the combined effect of these perturbations can be obtained by simply adding them together. Since no further perturbations occur in the chosen boxes, we can evolve these initial conditions to the present day using standard N-body techniques⁶.

As a final point, we address a technical question connected with applying the adhesion approximation to a model with HDM. In our HDM scenario, the evolution of density on any scale up to a redshift of 400 is described very well by linear gravity. This is because up to this time the density contrast averaged over an arbitrarily small volume is always less than or of order 0.01. After this time, the effects of non-linear gravity start to be important. Free streaming by neutrinos does not affect this non-linear evolution on any interesting scales, because the typical distance moved by a neutrino between this time and today is of order 0.2Mpc. So we only need to take HDM into account in the linear regime, and we can use standard cold N-body techniques to carry out the subsequent non-linear evolution.

⁶For speed, we perform the same evolution using the adhesion approximation. For our statistics we evolved 10 realizations of each model, with 32^3 particles on a 32^3 grid. The adhesion approximation has one free parameter, the viscosity, which we set to be (2 grid units)².

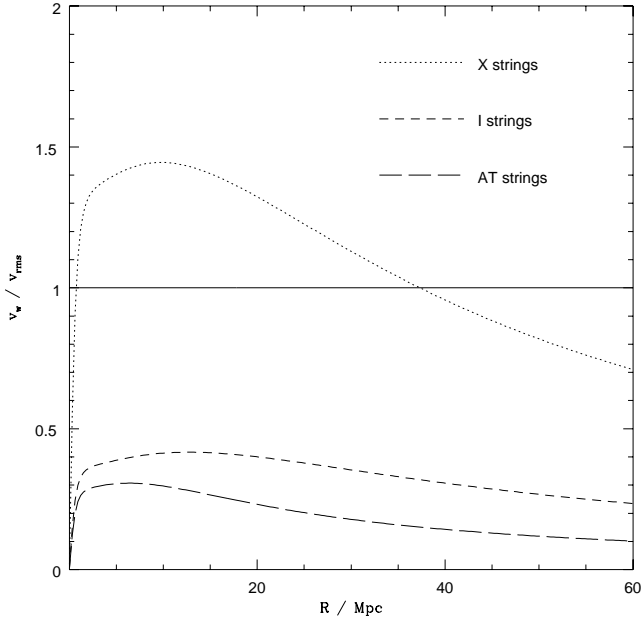


Figure 12: Graph showing the ratio v_W / v_{rms} as a function of sphere radius for spheres laid down on the edge of “maximal” wakes in the AT, I and X string models.

B A wake visibility criterion based on velocity coherence

In Section 2 we described a criterion based on linear gravity for testing whether cosmic string wakes stand out. Now, a simple alternative to linear gravity is given by the Zeldovich approximation, which gives a more realistic picture of the evolution of a distribution into the non linear regime. In the Zeldovich approximation, the evolution of the matter is determined by the *velocities* of test particles laid down in the initial density field. We might hope that an improvement on the linear gravity wakiness criterion would be provided by a similar “velocity coherence” criterion. Here, we ask whether the dominant contribution to the mean velocity of a sphere of radius R sitting on the edge of a wake comes from the wake (v_W) or from the Gaussian background (v_{rms}). If $v_W \geq v_{\text{rms}}$ then the wake may be said to stand out. We have

$$v_W = 8 \mu \Sigma (1 + z_{\text{eq}}) \times \int_0^\infty dk \frac{\sin kR}{k} w(kR) T(k, \eta_W) \quad (24)$$

$$v_{\text{rms}}^2 = 4 \pi \int_0^\infty dk |w(kR)|^2 P(k) \quad (25)$$

where $w(x)$ is the spherical window function used by Albrecht & Stebbins [2] and η_W is the time at which the wake in question has been laid down.

Results for this criteria for maximal wakes in the three models are given in Figure 12. Results for wakes laid down over a range of times in the X model are shown in Figure 13. It is seen that only the X wakes satisfy the velocity coherence criterion. That is, only X wakes dominate the bulk motions of nearby matter. Because of this, they will tend to stand out more and more as they undergo non-linear gravitational evolution. In a string model producing wakes of this type, the universe should contain high density sheets which directly track the motions of strings. On the other hand, wakes which do not satisfy the velocity coherence criterion will tend to break up and become less visible through non-linear evolution. These facts are borne out by an examination of the pictures in Section 2.2.

We expect that the velocity coherence criterion will provide a good test of whether wakes present in linear density fields will be visible in the universe today.

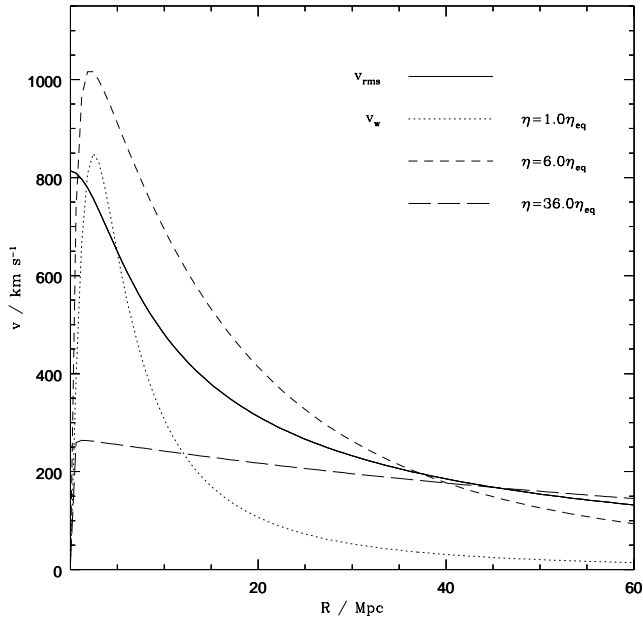


Figure 13: Graph showing v_{rms} and v_w as a function of sphere radius for spheres laid down on the edge of wakes in the X string model. Each dotted curve is for a wake laid down at a particular time. The velocities are normalized to the present day using linear gravity.

C Flatness of sections of a spherical shell

Strings are curved, and they move in curved paths. In the one scale model, the degree of curvature is characterized by a radius of curvature of order ξ . It is often useful to imagine that the sheets they trace out are spherical shells of radius ξ [11]. In order for our flatness statistic to pick out wakes, it must be sensitive to the flatness of sections of these shells. Figure 14 shows the value of the flatness quantities F and S_2 described in 3.2 for various sections of a spherical shell. Each section is constructed by cutting the sphere with a plane, and only considering that part of the sphere lying on one side of the cut. We quantify the shell fraction as the ratio of the area of the section to the area of the sphere. We observe that $F \geq 0.7$ for sections ranging from the planar limit to a half-sphere, whereas S_2 falls to 0.2 for a half-sphere. We anticipate that F may be more sensitive than S_2 for identifying wakes and other sheet-like features which do not start off exactly flat.

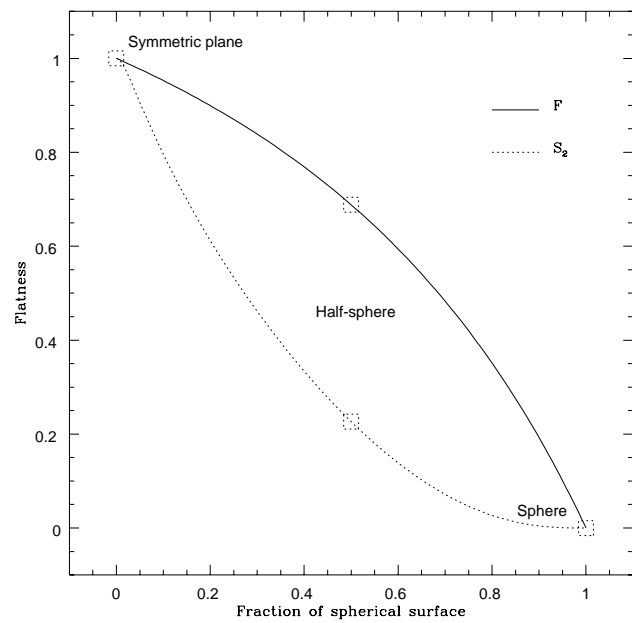


Figure 14: Graph showing the flatness of various fractions of a spherical shell.